NJC

Accepted Manuscript

This is an *Accepted Manuscript*, which has been through the Royal Society of Chemistry peer review process and has been accepted for publication.

Accepted Manuscripts are published online shortly after acceptance, before technical editing, formatting and proof reading. Using this free service, authors can make their results available to the community, in citable form, before we publish the edited article. We will replace this *Accepted Manuscript* with the edited and formatted *Advance Article* as soon as it is available.

You can find more information about *Accepted Manuscripts* in the Information for Authors.

Please note that technical editing may introduce minor changes to the text and/or graphics, which may alter content. The journal's standard Terms & Conditions and the Ethical guidelines still apply. In no event shall the Royal Society of Chemistry be held responsible for any errors or omissions in this *Accepted Manuscript* or any consequences arising from the use of any information it contains.

ROYAL SOCIETY OF CHEMISTRY

www.rsc.org/njc

New Journal of Chemistry

Dynamic Article Links ►

Cite this: DOI: 10.1039/c0xx00000x

www.rsc.org/xxxxxx

ARTICLE TYPE

Synthesis, structure, spectroscopy of four novel supramolecular complexes and cytotoxicity study by application of multiple parallel perfused microbioreactors

Qing-Lin Guan[a,b], Zhi Liu[b], Wen-Juan Wei[a], Jing Liu*[a], Yong-Heng Xing*[b], Rui Zhang[b], Ya-Nan Hou[b], Xuan Wang[b] and Feng-Ying Bai[b]

Received (in XXX, XXX) Xth XXXXXXXXX 20XX, Accepted Xth XXXXXXXXX 20XX

DOI: 10.1039/b000000x

Four novel supramolecular complexes $[Cd(H_2L)_2]\cdot(NO_3)_2\cdot 2H_2O$ (**1**), $[Cd(H_2L)_2]\cdot(OH)_2\cdot(EtOH)_{0.5}$ (**2**), $[Zn(H_2L)(2,6\text{-pdc})]\cdot(2,6\text{-}H_2pdc)_{1.5}\cdot MeOH\cdot 0.5H_2O$ (**3**) and $[Zn(H_2L)_2][Zn(2,5\text{-Hpdc})_3]_2\cdot 1.5H_2O$ (**4**) (H_2L = 2,6-di-(5-methyl-1H-pyrazol-3-yl)pyridine, 2,6-H_2pdc = 2,6-pyridinedicarboxylic acid, 2,5-H_2pdc = 2,5-pyridinedicarboxylic acid) based on pyrazolyl derivatives as ligands were designed and synthesized. They were characterized by elemental analysis, IR and UV-vis spectroscopy, powder X-ray diffraction and single-crystal X-ray diffraction. The structural analysis indicates that center metal atom (Cadmium and Zinc atoms) is a six-coordinated mode, and possess slightly distorted-octahedral configuration. In addition, the cytotoxicity study was performed by multiple parallel perfused microbioreactors and the potential apoptotic effects on PC12 cells and human adipose tissue-derived stem cells (hADSCs) were examined by flow-cytometric analysis. The results show that the percentage of apoptotic cells becomes gradually higher as increasing the concentration of supramolecular complex.

Introduction

In recent years, extensive investigations of the compounds containing N-heterocyclic ligand (e.g. pyrazole, pyridine, imidazole, etc.) and their derivatives have been focused on the field of coordination chemistry due to their good binding abilities[1]. Especially for pyrazole and its derivatives, they have attracted much attention of pharmacy experts for their good biological activity and compatibility[2]. They can not only be used as insecticides, fungicides, and herbicides, but also have anti-tumor properties[3]. With the characteristics of high efficiency and low toxicity, they can reduce the cost of pharmaceuticals and the environment contamination. As the simultaneous presence of Lewis basic donors and Lewis acid acceptors in the case of NH group from pyrazole, the versatility of the N-heterocyclic ligands is appropriate for forming different kinds of hydrogen bonds. They have been used for preparing supramolecular complex with many functions such as anionic sensing and hydrometallurgy[4]. There are two types of multi-dentate 2,6-di(pyrazolyl)pyridine ligands: 2,6-di(pyrazol-1-yl)pyridine and 2,6-di(pyrazol-3-yl)pyridine, where the pyrazole rings are introduced into the second and the sixth position of the pyridine ring, respectively. Although many complexes containing different 2,6-bis(pyrazolyl)pyridine were reported[5-7], the coordination chemistry about bipyrazole-pyridine derivatives has been paid less attention.

On the other hand, to our knowledge, since its discovery in 1936, 2,6-pyridine dicarboxylic acid (2,6-H_2pdc) has been widely used in a variety of processes as an enzyme inhibitor, plant preservative or food sanitize[8], and it is now known to be a major component (5-15% of the dry weight) of bacterial spores[9]. There is a rigid 120° angle between the central pyridine ring and the two carboxylate groups in 2,6-H_2pdc. Therefore, 2,6-H_2pdc could potentially provide various coordination modes to form either discrete or polymer metal complexes under appropriate synthesis conditions. In the meantime, 2,5-pyridinedicarboxylic acid (2,5-H_2pdc), with divergent function groups, could take more possibility to form bridging hydrogen bonds. Interestingly, that is potential for self-assembly[10]. The structure of 2,5-H_2pdc is suitable for the synthesis of cage materials because the two carboxylate groups in 2- and 5- ring position could easily coordinate to different metal centers, and the relative position of the coordinative moieties is adequate to form supramolecular structures with varied structural feature[11]. Furthermore, the complexes are also of great interest due to their potential applications in many areas, such as enzyme inhibitor[12], antibacterial activity[13], catalysis[14] and fluorescent[15–17]. Many complexes containing 2,6-H_2pdc/2,5-H_2pdc ligand have been reported[18-20]. However, the complexes with mixed ligands of 2,6-H_2pdc/2,5-H_2pdc and 2,6-di-(pyrazolyl)pyridine have seldom been reported. In addition, participation of transition metal compounds in biological activity research has received tremendous interest in the past decades[21-25].

Nowadays, metal-based pharmaceuticals emerging from the interface of inorganic chemistry, pharmacology, toxicology and biochemistry have witnessed spectacular successes, and the discovery of the cytotoxic properties of metal ions has provided

enormous impetus for research into the use of metal complexes in the fight against disease. A broad array of medicinal applications of these compounds has been investigated, and some of them are found to be useful both as clinical diagnostic agents and in chemotherapeutic applications. In addition, stem cells, which are pluripotent cells for self-renewing, have attracted wide attention for study. They are able to differentiate multiple cell lineages under appropriate conditions. Thus, they have been used for a variety of therapeutic applications[26]. A recent study from Harvard University showed that kenpaullone are more effective and cheaper than current drugs for Amyotrophic Lateral Sclerosis (ALS) by a new type of stem-cell-based motor neuron screen[27]. Moreover, the adrenal phaeochromocytoma (PC12) cell line was originally isolated from a tumour in the adrenal medulla of a rat in 1976[28]. PC12 cells resemble the phenotype of sympathetic ganglion neurons upon differentiation with nerve growth factor (NGF) and can be subcultured indefinitely. PC12 cells and human adipose tissue-derived stem cells (hADSCs) were chosen to test cytotoxicity for evaluating whether these complexes could potentially be used as drug precursors or not.

In our present work, four superamolecular complexes $[Cd(H_2L)_2]\cdot(NO_3)_2\cdot 2H_2O$ (**1**), $[Cd(H_2L)_2]\cdot(OH)_2\cdot(EtOH)_{0.5}$ (**2**), $[Zn(H_2L)(2,6\text{-pdc})]\cdot(2,6\text{-}H_2pdc)_{1.5}\cdot MeOH\cdot 0.5H_2O$ (**3**) and $[Zn(H_2L)_2][Zn(2,5\text{-Hpdc})_3]_2\cdot 1.5H_2O$ (**4**) (H_2L = 2,6-bis(5-methyl-1H-pyrazol-3-yl)pyridine) were synthesized for the first time under hydrothermal conditions. The spectral and structural characterizations of these supramolecular complexes were conducted and their cytotoxicity toward hADSCs was evaluated using multiple parallel perfused microbioreactors[29]. The cytotoxicity of the four complexes has been evaluated by MTT (MTT = (3-(4,5-dimethylthiazol-2-yl)-2,5-diphenyltetrazolium bromide)) assay as well. The apoptosis of hADSCs cells induced by the supramolecular complexes was also studied.

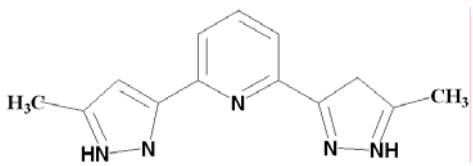

Scheme 1 Structure of the H_2L

Experiment

Materials and methods

Elemental analysis was performed with a PE 240C automatic analyzer (Perkin-Elmer, Waltham, MA). IR spectra were determined with a FT/IR-480 PLUS Fourier Transform spectrometer (JASCO, Tokyo, Japan) (200-4000 cm-1, with pressed KBr pellets). UV–vis spectra were recorded with a V–570-UV/VIS/NIR spectrophotometer (JASCO, Tokyo, Japan) (200-2500 nm, in the form of the solid sample). Fluorescence spectra were determined with a FP-6500 spectrofluorimeter (JASCO, Tokyo, Japan) (200-800 nm). X-ray powder diffraction (PXRD) patterns were performed on a Bruker AXS SMART Ⅱ CCD (Bruker AXS, Germany). H_2L was synthesized according to the modified literature method[30]. All chemicals used were analytical grade, except for dimethylsulfoxide (DMSO) that was cell culture grade. MTT [3-(4,5-dimethylthiazol-2-yl)-2,5-diphenyl tetrazolium bromide] was purchased from Sigma Corporation, USA. PC12 cells and human ADSCs were donated by the Regenerative Medicine Centre in First Affiliated Hospital of Dalian Medical University.

Synthesis of $[Cd(H_2L)_2]\cdot(NO_3)_2\cdot 2H_2O$ (1) $Cd(NO_3)_2\cdot 4H_2O$ (0.031 g, 0.1 mmol) and H_2L (0.023 g, 0.1 mmol) in MeOH (8 mL) were mixed in 20 mL beaker and stirred for 5 h, the final reaction mixture was sealed in a 25 mL Teflon-lined stainless steel vessel under autogenous pressure and heated at 160 °C for 3 days, then followed by slow cooling to room temperature. White block crystals suitable for X-ray diffraction analysis were obtained. Yield: 0.047 g (0.06 mmol), 63%. Anal. Calc. for $C_{26}H_{28}N_{12}O_8Cd$ (751.02): C, 41.54; H, 3.73; N, 22.37%. Found: C, 41.62; H, 3.69; N, 22.39. IR data (KBr, cm-1): 3417, 3191, 3127, 2932, 2859, 1610, 1582, 1447, 1293, 1011.

Synthesis of $[Cd(H_2L)_2]\cdot(OH)_2\cdot(EtOH)_{0.5}$ (2) $Cd(NO_3)_2\cdot 4H_2O$ (0.032 g, 0.1 mmol) and H_2L (0.024 g, 0.1 mmol) in water (6 mL) and EtOH (4 mL) were mixed in a 25mL beaker and stirred for 5 h, the final reaction mixture was sealed in a 25 mL Teflon-lined stainless steel vessel under autogenous pressure and heated at 160 °C for 3 days, then followed by slow cooling to room temperature. White block crystals suitable for X-ray diffraction analysis were obtained. Yield: 0.036 g (0.06 mmol), 55%. Anal. Calc. for $C_{27}H_{31}N_{10}O_{2.5}Cd$ (648.02): C, 50.00; H, 4.78; N, 21.60%. Found: C, 49.95; H, 4.84; N, 21.57. IR data (KBr, cm-1): 3437, 3195, 3128, 2925, 2858, 1581, 1508, 1446, 1326, 1014.

Synthesis of $[Zn(H_2L)(2,6\text{-pdc})]\cdot(2,6\text{-}H_2pdc)_{1.5}\cdot MeOH\cdot 0.5H_2O$ (3) $Zn(OAc)_2\cdot 2H_2O$ (0.022 g, 0.1 mmol), H_2L (0.024 g, 0.1 mmol) and 2,6-H_2pdc (0.051 g, 0.3 mmol) in water (6 mL) and MeOH (4 mL) were mixed in a 25mL beaker and stirred. After 5 h, the final reaction mixture was sealed in a 25 mL Teflon-lined stainless steel vessel under autogenous pressure and heated at 160 °C for 3 days, then followed by slow cooling to room temperature. Colorless block crystals suitable for X-ray diffraction analysis were obtained. Yield: 0.034 g (0.04 mmol), 58%. Anal.Calc. for $C_{31.5}H_{28.5}N_{7.5}O_{11.5}Zn$ (761.49): C, 49.64; H, 3.74; N, 13.79%. Found: C, 49.69; H, 3.68; N, 13.75. IR data (KBr, cm-1): 3456, 3136, 3085, 2929, 2858, 1519, 1446, 1290, 1253, 1018, 1620, 1380.

Synthesis of $[Zn(H_2L)_2][Zn(2,5\text{-Hpdc})_3]_2\cdot 1.5H_2O$ (4) $Zn(OAc)_2\cdot 2H_2O$ (0.021 g, 0.1 mmol), H_2L (0.024 g, 0.1 mmol) and 2,5-H_2pdc (0.050 g, 0.3 mmol) in water (6 mL) and MeOH (4 mL) were mixed in a 25mL beaker and stirred. After 5 h, the final reaction mixture was sealed in a 25 mL Teflon-lined stainless steel vessel under autogenous pressure and heated at 160 °C for 3 days, then followed by slow cooling to room temperature. Colorless block crystals suitable for X-ray diffraction analysis were obtained. Yield: 0.035 g (0.02 mmol), 62%. Anal.Calc. for $C_{68}H_{53}N_{16}O_{25.5}Zn_3$ (1698.43): C, 48.04; H, 3.12; N, 13.20%. Found: C, 47.98; H, 3.15; N, 13.12. IR data (KBr, cm-1): 3445 3167, 3025, 2923, 2853, 1559, 1508, 1457, 1261, 1038, 1640, 1399.

The crystals of complexes **1-4** were difficult to dissolve in water and common organic solvents except for DMSO and dimethylformamide (DMF).

X-ray Crystallographic Determination

Suitable single crystals of the three supramolecular complexes were mounted on glass fibers for X-ray measurement. Reflection

data was collected at room temperature on Bruker AXS SMART APEX II CCD diffractometer with graphite-monochromated Mo-Ka radiation (λ=0.7107 Å) and a ω scan mode. All the measured independent reflections (I > 2 σ (I)) were used in the structural analysis, and semi-empirical absorption corrections were applied using SADABS program[31]. The structures were solved by the direct method using SHELXL-97[32]. Crystal data and structure refinements are shown in **Table 1**. Hydrogen bond lengths (Å) and angles (°) are shown in **Table 2**. All non-hydrogen atoms were refined anisotropically and the temperature factors were processed by full-matrix least squares method. Hydrogen atoms of the organic frameworks were fixed at calculated positions geometrically and refined by a riding model, whereas hydrogen atoms of the lattice water molecules were found in the different Fourier maps. The value of the Flack[33] parameter is 0.44(5) for the complex **1** and 0.17(6) for complex **2**, respectively. For supramolecular complex **1**, it was found that oxygen atoms of one lattice NO_3^- was disordered and modeled over two split positions with occupancies in ratio of 0.5:0.5, for O4(O4B), O5(O5B) and O6(O6B), respectively. For supramolecular complex **4**, the affiliated H atoms of O2W were not located in the different Fourier maps.

Table 1 Crystallographic data for the supramolecular complexes **1**-**4**.

Complex	**1**	**2**	**3**	**4**
Formula	$C_{26}H_{30}N_{12}O_8Cd$	$C_{27}H_{31}N_{10}O_{2.5}Cd$	$C_{31.5}H_{28.5}N_{7.5}O_{11.5}Zn$	$C_{68}H_{53}N_{16}O_{25.5}Zn_3$
M(g mol^{-1})	751.02	648.02	761.49	1698.43
Crystal system	Tetragonal	Tetragonal	Triclinic	Monoclinic
Space group	*P41*	*P41*	*P-1*	*$P2_1/c$*
a(Å)	9.807 (9)	9.839 (1)	9.537(4)	9.9875(7)
b(Å)	9.807 (9)	9.839(1)	12,679 (3)	21.4600(18)
c(Å)	34.426(3)	34.516(3)	15.191(1)	34.472(3)
α(º)	90	90	108.093(1)	90
β(º)	90	90	104.845(1)	104.236(5)
γ(º)	90	90	91.562(1)	90
V(Å^3)	3311.6(3)	3341.4(4)	1676.42(19)	7161.6(10)
Z	4	4	2	4
D_{calc}(g.cm^{-3})	1.506	1.288	1.509	1.575
Crystal size (mm)	0.49×0.28×0.20	0.51×0.29×0.21	0.53×0.33×0.22	0.28×0.21×0.07
F(000)	1528	1324	784	3468
μ(Mo-Kα)/mm^{-1}	0.724	0.693	0.807	1.091
θ (°)	2.08-28.22	2.07-28.72	1.85-26.73	1.13-23.35
Reflections collected	20673	20559	9720	34483
Independent reflections (I >2σ(I))	7950	8100	6968	10369
Parameters	457	393	542	1028
Flack parameter	0.44(5)	0.17(6)	-	-
Limiting indices	-11≤h≤13 -13≤k≤6 -43≤l≤43	-13≤h≤13 -6≤k≤13 -46≤l≤44	-11≤h≤12 -16≤k≤15 -19≤l≤14	-11≤h≤11 -23≤k≤14 -38≤l≤34
Goodness of fit	1.071	1.052	1.029	0.857
R[a]	0.0771(0.0951)[b]	0.0889(0.1139)[b]	0.0390(0.0563)[b]	0.0613(0.1699)[b]
wR_2[a]	0.1780(0.1885)[b]	0.2475 (0.2706)[b]	0.0922(0.1008)[b]	0.1529(0.1842)[b]

$\Delta(\rho)(e\text{Å}^{-3})$	0.812 and -1.411	2.063 and -0.825	0.494 and -0.366	1.655 and -0.493

[a] $R = \Sigma ||Fo| - |Fc|| / \Sigma |Fo|$, $wR_2 = [\Sigma (w (Fo^2 - Fc^2)^2 / \Sigma (w (Fo^2)^2]^{1/2}$; [$Fo > 4\sigma (Fo)$].

[b] Based on all data.

Table 2 Hydrogen bond lengths (Å) and angles (°) for complexes **1-4***

D–H···A	d(D–H)/Å	d(H···A)/Å	d(D···A)/Å	∠D–H···A/°
		Complex **1**		
O1W—H1A---O4$^{\#1}$	0.79	2.12	2.83(3)	147
O2W—H2A---O2	0.82	2.28	3.097(5)	177
N6—H6---O5	0.86	2.27	3.081(2)	156
N6—H6---O6	0.86	2.31	3.088(4)	150
N10—H10A---O1W	0.86	1.93	2.779(5)	171
C11—H11---O1$^{\#2}$	0.93	2.54	3.260(2)	134
C14—H14B---O3$^{\#3}$	0.96	2.43	3.237(9)	142
C21—H21---O4$^{\#4}$	0.93	2.56	3.31(3)	137
C24—H24---O4$^{\#4}$	0.93	2.55	3.31(3)	138
		Complex **2**		
N1—H1D---O5$^{\#1}$	0.86	1.85	2.712(9)	174
N5—H5---O1	0.86	2.18	2.934(9)	147
N6—H6A---O3	0.86	1.97	2.810(7)	163
		Complex **3**		
O5—H5B---O4$^{\#1}$	0.82(8)	1.67(6)	2.503(3)	178(5)
O7—H7A---O9	0.94(4)	1.65(4)	2.581(3)	173(4)
O9—H9---O12	0.82	2.22	3.032(7)	170
O10—H10A---O1	0.85	1.68	2.507(4)	163
N1—H1---O8	0.83(3)	2.55(3)	3.051(3)	120(2)
N5—H5A---O6$^{\#2}$	0.80(3)	2.13(3)	2.853(3)	150(3)
C7—H7B---O8$^{\#3}$	0.93	2.38	3.155(3)	141
C24—H24B---O11$^{\#4}$	0.93	2.33	3.231(5)	162
C24—H24B---O13$^{\#5}$	0.93	2.38	3.263(5)	157
N1—H1---N7	0.83(3)	2.24(3)	3.051(3)	167(3)
		Complex **4**		
O2—H2---O1W$^{\#1}$	0.82	2.17	2.804(15)	134
O5—H5---O23$^{\#2}$	0.82	1.77	2.565(9)	162
O9—H9---O16	0.82	1.82	2.612(9)	162
O21—H21---O4	0.82	1.84	2.625(9)	158
N1—H1A---O15$^{\#3}$	0.86	2.03	2.876(10)	169
N5—H5A---O20$^{\#4}$	0.86	1.99	2.762(10)	150
N6—H6A---O11$^{\#5}$	0.86	1.91	2.758(10)	168

N10—H10A---O8$^{\#6}$	0.86	2.06	2.907(10)	168
C16—H16A---O23$^{\#3}$	0.93	2.48	3.378(11)	162
C36—H36A---O22	0.93	2.29	3.165(12)	156

*Symmetry transformation used to generate equivalent atoms: complex **1**: #1=x+1,y,z; #2=x,y-1,z; #3=x-1,-y, z+1/4; #4=x,1-y, z+1/4; complex **2**: #1=x,y-1,z; complex **3**: #1=2-x,-y,1-z; #2=x-1,y,z; #3=1-x,-y,1-z; #4=2-x,1-y,2-z; #5=x,y,1+z; complex **4**: #1=x, y+1,z; #2=-x,1/2+y,1/2-z; #3=1-x,y+1/2,1/2-z; #4=1+x,y,z; #5=x+1,3/2-y,z-1/2; #6=x,3/2-y,z-1/2.

Cell Cultures

PC12 cells were maintained at a density of 3×10^7 cells/cm^2 in 25 cm^2 flasks Roswell Park Memorial Institute - 1640 (RPMI-1640; Gibco, USA) and supplemented with 10 % fetal bovine serum (FBS; Gibco, USA)) and 1 % penicillin and streptomycin (Gibco, USA). Human ADSCs were maintained at a density of 3×10^7 cells/cm^2 in 25 cm^2 flasks in Human Adipose-Derived Mesenchymal Stem Cell Basal Medium (Cyagen, USA) containing 10 % Adipose-Derived Mesenchymal Stem Cell-Qualified Fetal Bovine Serum (Cyagen, USA), 1 % Penicillin-Streptomycin (Cyagen, USA) and 1 % Glutamine (Cyagen, USA). All cells were cultured at 37 ºC in a 5 % CO_2 atmosphere for 72 h and non-adherent cells were removed. Cells were trypsinized (0.25 % trypsin - 0.02 % EDTA; Invitrogen, USA), harvested and re-plated at a ratio of 1:2 or 1:3 in new culture flasks, when cells reached 70~80% confluence.

Complexes **1-4** were first solubilized in DMSO at concentrations not exceeding 0.1 % and then diluted in cell culture medium.

MTT cell viability assay

Cytotoxicity of supramolecular complexes 1-4 was evaluated by using standard MTT (3-(4,5-dimethylthiazole)-2,5-diphenyltetraazolium bromide) assay[34]. MTT was dissolved in phosphate buffered saline (PBS) solution at a concentration of 5 mg/ml, filtered through a 0.22 μM filter to sterilize and to remove the insoluble residues, then the MTT solution was stored in the amber vials at 4^o C. The stock solution was diluted to the desired concentrations immediately before using.

PC12 cells and human ADSCs were placed in 96-well microassay culture plates (1000 cells/well) respectively and grown overnight at 37 ^{o}C in a 5% CO_2 incubator. The tested supramolecular complexes were then added to the wells to achieve final concentrations of 0.025, 0.05, 0.1, 0.2, 0.4, 0.8 and 1.6 mM. Each experiment contained one control only treated by culture medium. The plates were incubated at 37 ºC in a 5% CO_2 incubator for 24 h / 48 h. Then, 100 μl/well of MTT solution (5 mg/ml) was added, and the plates were incubated for another 4 h. Supernatants were removed and formazan crystals were solubilized in 150 μl of dimethylsulfoxide (DMSO; Sigma, USA). Optical densities (OD) were determined at 490 nm using a microplate reader (BioTek EL808, USA).

The cell viability was calculated using the following equation:

Cell viability (%) = OD value of treated well / OD value of the control × 100.

Microbioreactors for parallel screening

Cells were also conducted in 4-well TissueFlex® (Zyoxel Ltd, UK) microbioreactors (**Fig. 1**) for parallel screening. Briefly, cells were plated at 2.4×10^6 cells/cm^2 onto the surface of the microbioreactor, which was coated with 0.01% poly-L-lysine (Sigma, St Louis, MO), and cultured under perfusion conditions at 37 ºC. Culture medium was supplied continuously by a multi-channel peristaltic pump or by syringe pumps at 0.5 μL/min. After 48h, cells morphologic changes were observed with an inverted microscope.

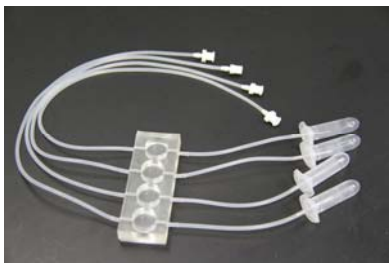

Fig. 1 The multiple parallel perfused microbioreactor (TissueFlex®) used for experiments.

Apoptosis assay

Apoptosis assay was performed with double staining utilizing acridine orange (AO) and ethidium bromide (EB)[35]. On the basis of overall cell morphology and cell membrane integrity, necrotic and apoptotic cells can be distinguished. AO can pass through intact cell membrane, while EB only penetrates into damaged cell membranes. Under fluorescence microscope, live cells appear green fluorescence. Necrotic cells appear reddish-orange fluorescence having similar nuclear morphology with viable cells. Apoptosis cells also appear green fluorescence, however, morphological change such as cell blebbing and formation of apoptotic bodies could be observed.

AO (Sigma A-6014, USA) or EB (Sigma E-8751, USA) were adjusted to 100 mg/L in PBS and 4 μL was added into 100 μL of cell suspension followed by gentle mixing. After 48 h, each cell culture was stained with AO/EB solution. Fluorescent images were observed using a fluorescence microscope (Leica DMI 6000B, Berlin, Germany) equipped with a CoolSNAP-EZ CCD-camera (Leica DFC 500, Berlin, Germany). At least five images were randomly chosen.

Human ADSCs were seeded in 6-well plates (2×10^5 cells/well) in duplicate and cultured overnight, after which the tested drugs were added. For cell apoptosis analysis, the drugs were diluted at concentrations of 0.025, 0.1, 0.4 and 1.6 mM. Following treatment with the drugs, hADSCs apoptosis was evaluated with an Annexin V–FITC–fluorescein isothiocyanate apoptosis detection kit (BD Biosciences, USA) and analyzed with a flow cytometer (FACS Calibur Becton Dickinson, San Jose, CA) using Cell Quest software.

Statistical analysis

All data were expressed as mean ± standard deviations. Analysis of variance was performed with SPSS 13.0 software to determine significant differences among groups. Mean values and standard deviations were calculated for each sample examined in at least three independent experiments. P-values < 0.05 were considered significant.

Results and discussion

Description of the crystal structure

The structure of $[Cd(H_2L)_2]\cdot(NO_3)_2\cdot 2H_2O$ (1) X-ray diffraction analysis revealed that the asymmetric unit of supramolecular complex **1** consisted of one Cd atom, two H_2L ligands, two lattice NO_3^- anions and two lattice H_2O molecules. The coordination environment of the central Cd atom in **1** was shown in **Fig. 2a** with atom numbering. The Cd atom is six-coordinated by six nitrogen atoms (N2, N3, N4, N7, N8 and N9) from two H_2L ligands with Cd-N bond distances in the range of 2.295(8)-2.373(9) Å, to form a distorted octahedron geometry.

The deviations of N3, N7, N8 and N9 atoms that composed of the least-squares plane are 0.0016, -0.0023, 0.0031 and -0.0024 Å, respectively, showing that these atoms are almost on one plane. The Cd, N2 and N4 from the axial position lay 0.0362, -2.1763 and 2.2082 Å out of the equatorial plane, indicating that Cd toward the N4, trans to N2. The angles of the N-Cd-N are in the range of 68.1(3)~173.91(2)°. In the structure of **1**, H_2L ligand was coordinated to Cd atom by the tridentate coordination mode with $\mu_1-\eta^1-\eta^1-\eta^1$ chelating fashion, namely, two N atoms from two pyrazolyl rings, one N atom from one pyridine ring.

There are three kinds of hydrogen bonds in supramolecular complex **1**: (1) hydrogen bond (O—H---O) between the oxygen (donor) and oxygen (acceptor) includes O1W—H1A---O4$^{\#1}$, O2W—H2A---O2 (O1W and O2W from lattice waters, O2 and O4 from lattice NO_3^- anions); (2) hydrogen bond (N—H---O) between the nitrogen (donor) and oxygen (acceptor) includes N6—H6---O5, N6—H6---O6 and N10—H10A---O1W (N6 and N10 from uncoordinated nitrogen from H_2L ligand, O5 and O6 from lattice NO_3^- anions, O1W from lattice water); (3) hydrogen bonds (C—H---O) of carbon (donor) from H_2L ligands and the oxygen (acceptor) from lattice NO_3^- anions: C11—H11---O1$^{\#2}$, C14—H14B---O3$^{\#3}$, C21—H21---O4$^{\#4}$ and C24—H24---O4$^{\#5}$. The adjacent molecular units are further connected, to form a 1D chain (**Fig. 2b**) by the hydrogen bonds of C21—H21---O4$^{\#4}$, C24—H24---O4$^{\#5}$, N6—H6---O5 and N6—H6---O6. The two adjacent chains are linked to form a 2D layer (**Fig. 2c**) by the hydrogen bond of C11—H11---O1$^{\#2}$ and C14—H14B---O3$^{\#3}$. The two adjacent layers were connected to form a 3D supramolecular network structure (**Fig. 2d**) by the hydrogen bond of O1W—H1A---O4$^{\#1}$, O2W—H2A---O2 and N10—H10A---O1W.

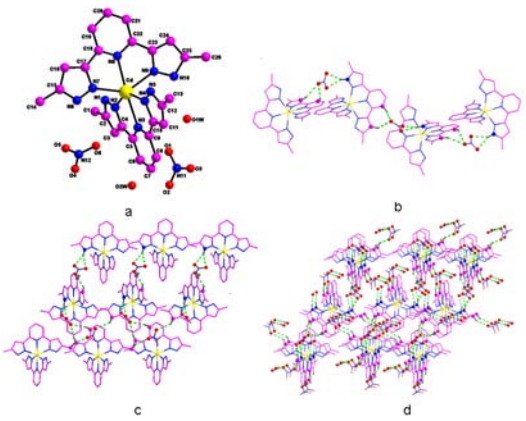

Fig. 2 The molecular structure of supramolecular complex **1** (a); 1D chain via hydrogen bonds (b); 2D layer via hydrogen bonds (c); 3D supramolecular network structure via hydrogen bonds (d).

The structure of $[Cd(H_2L)_2]\cdot(OH)_2\cdot(EtOH)_{0.5}$ (2) X-ray diffraction analysis revealed that the asymmetric unit of supramolecular complex **2** consisted of one Cd atom, two H_2L ligands, two lattice OH- anions and a half lattice EtOH molecule. The coordination environment of the central Cd atom in **2** is shown in Fig**. 3** with atom numbering. The Cd atom is six-coordinated by six nitrogen atoms (N2, N3, N4, N7, N8 and N9) from two H_2L ligands with Cd-N bond distances in the range of 2.24(2)-2.366(9)Å, to form a distorted octahedron geometry. The deviations of N3, N7, N8 and N9 atoms that composed of the least-squares plane are 0.0034, -0.0052, 0.0067 and -0.0050 Å, respectively, showing that these atoms are almost on one plane. The Cd, N2 and N4 from the axial position lay 0.0110, 2.2409 and -2.1884 Å out of the equatorial plane, indicating that Cd toward the N4, trans to N2. The angles of the N-Cd-N are in the range of 68.1(3)~175.2(3)°. In the structure, H_2L ligand was coordinated to Cd atom by the tridentate coordination mode with $\mu_1-\eta^1-\eta^1-\eta^1$ chelating fashion, namely, two N atoms from two pyrazolyl rings, one N atom from one pyridine ring. The only difference of **1** and **2** is free moieties, **1** is NO_3^- anion and water, while **2** is OH- anion and EtOH.

There is one kind of hydrogen bonds in supramolecular complex **2**: hydrogen bond (N—H---O) of nitrogen (donor) from H_2L ligand and oxygen (acceptor) from lattice OH^- anions and lattice EtOH molecule, respectively.

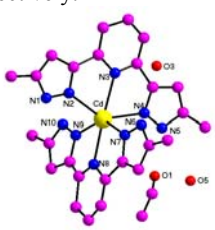

Fig. 3 The molecular structure of supramolecular complex **2.**

The structure of $[Zn(H_2L)(2,6\text{-}pdc)]\cdot(2,6\text{-}H_2pdc)_{1.5}\cdot MeOH\cdot 0.5H_2O$ (3) X-ray diffraction analysis revealed that the asymmetric unit of complex **3** consisted of one Zn atom, one H_2L ligand, one 2,6- H_2pdc ligand, one and a half lattice 2,6-H_2pdc molecule and a half lattice H_2O molecule. The

coordination environment of the central Zn atom in **3** is shown in **Fig. 4a** with atom numbering. The Zn atom is six-coordinated by four nitrogen atoms (N2, N3, N4 from H_2L ligand; N6 from 2,6-H_2pdc ligand) with Zn—N bond distances in the range of 2.0269(17)~2.241(2) Å, two oxygen atoms (O2, O3) from 2,6-H2pdc ligand with Zn—O bond length of 2.2155(15) ~2.2206(16) Å, to form a distorted octahedron geometry. The deviations of O2, O3, N3 and N6 atoms that composed of the least-squares plane are -0.0512, -0.0551, 0.0384 and 0.0679 Å, respectively, showing that these atoms are almost on one plane. The Zn, N2 and N4 from the axial position lay -0.0709, -2.1461 and 2.1155 Å out of the equatorial plane, indicating that Zn toward the N2, trans to N4. The angles of the O-Zn-O, O-Zn-N and N-Zn-N are in the range of 91.75(8)~151.32(6)°, 75.56(6)~109.92(6)° and 74.54(8)~170.98(8)°, respectively. In the structure, H_2L ligand is coordinated to Zn atom by the tridentate coordination mode with μ_1–η^1–η^1–η^1 chelating fashion, namely, two N atoms from two pyrazolyl rings, one N atom from one pyridine ring. 2,6-H_2pdc ligand was doordinated to Zn atom by the same coordination mode with μ_1–η^1–η^1–η^1 chelating fashion, namely, two O atoms from carboxylate group of the 2,6-H_2pdc ligand, one N atom from one pyridine ring.

There are four kinds of hydrogen bonds in the complex **3**: (1) hydrogen bond (O—H---O) between the oxygen (donor) and oxygen (acceptor) includes O5—H5B---O4$^{\#1}$, O7—H7A---O9, O9—H9---O12 and O10—H10A---O1 (O1 and O4 from uncoordinated oxygen from 2,6-H_2pdc ligand, O5, O7, O10 and O12 from lattice 2,6-H_2pdc ligands, O9 from lattice MeOH molecule); (2) hydrogen bond (N—H---O) between the nitrogen (donor) and oxygen (acceptor) includes N1—H1---O8 and N5—H5A---O6$^{\#2}$ (N1 and N5 from uncoordinated nitrogen from H_2L ligand, O6 and O8 from lattice 2,6-H_2pdc molecules); (3) hydrogen bonds (C—H---O) between the carbon (donor) and the oxygen (acceptor) includes: C7—H7B---O8$^{\#3}$, C24—H24B---O11$^{\#4}$ and C24—H24B---O13$^{\#5}$ (C7 from H2L ligand, C24 from lattice 2,6-H_2pdc molecule, O8, O11 and O13 from lattice 2,6-H_2pdc molecules); (4) hydrogen bond (N—H---N) between the nitrogen (donor) and the nitrogen (acceptor) includes N1—H1---N7 (N1 from uncoordinated nigrogen from H_2L ligand, N7 from lattice 2,6-H_2pdc molecule). The adjacent molecular units are further connected, to form a 1D chain (**Fig. 4b**) by the hydrogen bonds of N1—H1---O8 and N5—H5A---O6$^{\#2}$. The two adjacent chains are linked to form a 2D layer (**Fig. 4c**) by the hydrogen bond of N1—H1---N7, C7—H7B---O8$^{\#3}$ and O5—H5B---O4$^{\#1}$. The two adjacent layers were connected to form a 3D supramolecular network structure (**Fig. 4d**) by the hydrogen bond of O7—H7A---O9, O9—H9---O12, O10—H10A---O1, C24—H24B---O11$^{\#4}$ and C24—H24B---O13$^{\#5}$.

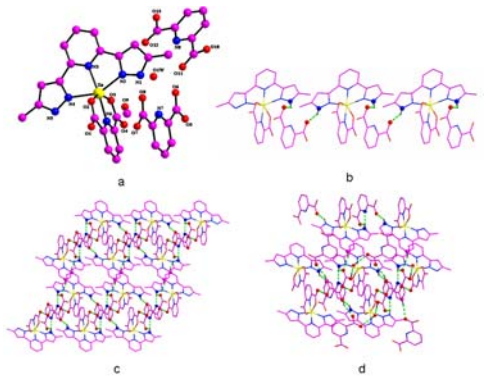

Fig. 4 The molecular structure of supramolecular complex **3** (a); 1D chain via hydrogen bonds (b); 2D layer via hydrogen bonds (c); 3D supramolecular network structure via hydrogen bonds (d).

The structure of $[Zn(H_2L)_2][Zn(2,5\text{-}Hpdc)_3]_2\cdot 1.5H_2O$ (4) X-ray single crystal analysis indicates that the complex **4** is crystallized in monoclinic system with $P2_1/c$ space group. In the asymmetric unit of the complex **4**, there are a $[Zn(H_2L)_2]^{2+}$ cation moiety, two $[Zn(2,5\text{-}Hpdc)_3]^-$ anions moiety and one and a half lattice H_2O molecule. In $[Zn(H_2L)_2]^{2+}$, including one Zn atom and two H_2L ligands, in $[Zn(2,5\text{-}Hpdc)_3]^-$, including one Zn atom and three 2,5-H_2pdc ligands.

The coordination environment of the three central Zn atoms in **4** is shown in **Fig. 5a** with atom numbering. The Zn1 atom is six-coordinated by six nitrogen atoms (N2, N3, N4, N7, N8 and N9) from two H_2L ligands with Zn1—N bond distances in the range of 2.056(7)-2.199(7) Å, to form a distorted octahedron geometry. The deviations of N3, N7, N8 and N9 atoms that composed of the least-squares plane are -0.0129, 0.0170, -0.0221 and 0.0180 Å, respectively, showing that these atoms are almost on one plane. The Zn1, N2 and N4 from the axial position lay 0.0266, -2.1122 and 2.0668 Å out of the equatorial plane, indicating that Zn1 toward the N4, trans to N2. The Zn2 atom is six-coordinated by three nitrogen atoms and three oxygen atoms (N11, N12, N13, O4, O8 and O12) from three 2,5-H_2pdc ligands with Zn2-N bond distances in the range of 2.166(7)—2.181(7)Å and with Zn2-O bond distances in the range of 2.056(7)-2.133(6)Å, to form a distorted octahedron geometry. The Zn3 atom is six-coordinated by three nitrogen atoms and three oxygen atoms (N11, N12, N13, O4, O8 and O12) from three 2,5-H_2pdc ligands with Zn3-N bond distances in the range of 2.101(8)-2.168(8) Å and with Zn3—O bond distances in the range of 2.071(7)-2.115(6) Å, to form a distorted octahedron geometry. The angles of the O−Zn−O, O−Zn−N and N−Zn−N are in the range of 89.2(3)~175.4(3)°, 76.3(3)~168.7(3)° and 75.2(3)~173.6(3)°, respectively.

In the structure of **4**, H_2L ligand is coordinated to Zn atom by the tridentate coordination mode with μ_1–η^1–η^1–η^1 chelating fashion, namely, two N atoms from two pyrazolyl rings, one N atom from one pyridine ring. 2,5-H_2pdc ligand is doordinated to Zn atom by the same coordination mode with μ_1–η^1–η^1 chelating fashion, namely, one O atom from carboxylate group of the 2,5-H_2pdc ligand, one N atom from one pyridine ring.

There are three kinds of hydrogen bonds in supramolecular complex **4**: (1) hydrogen bond (O—H---O) between the oxygen (donor) and oxygen (acceptor) includes O2—H2---O1W$^{\#1}$,

O5—H5---O23$^{\#2}$, O9—H9---O16 and O21—H21---O4 (O2, O5, O9, O21 and O23 from uncoordinated oxygen from 2,5-H_2pdc ligands, O4 and O16 from coordinated oxygen 2,5-H_2pdc ligands, O1W from lattice water molecule, #1=1-x,1-y,-z, #2=2-x,1/2+y,1/2-z); (2) hydrogen bond (N—H---O) between the nitrogen (donor) and oxygen (acceptor) includes N1—H1A---O15$^{\#3}$, N5—H5A---O20$^{\#4}$, N6—H6A---O11$^{\#5}$ and N10—H10A---O8$^{\#6}$ (N1, N5, N6 and N10 from uncoordinated nitrogen from H_2L ligands, O11, O15 and O20 from uncoordinated oxygen from 2,5-H_2pdc ligands, O8 from coordinated oxygen from 2,5-H_2pdc ligand); (3) hydrogen bonds (C—H---O) between the carbon (donor) and the oxygen (acceptor) includes: C16—H16A---O23$^{\#3}$ and C36—H36A---O22 (C16 from H2L ligand, C36 from 2,5-H_2pdc ligand, O22 and O23 from uncoordinated oxygen from 2,5-H_2pdc ligands). The adjacent molecular units are further connected, to form a 1D chain (Fig. **5b**) by the hydrogen bonds of O5—H5---O23$^{\#2}$, N1—H1A---O15$^{\#3}$, N5—H5A---O20$^{\#4}$, N10—H10A---O8$^{\#6}$ and O21—H21---O4. The two adjacent chains are linked to form a 2D layer (**Fig. 5c**) by the hydrogen bonds of C16—H16A---O23$^{\#3}$ and C36—H36A---O22. The two adjacent layers were connected to form a 3D supramolecular network structure (**Fig. 5d**) by the hydrogen bonds of O2—H2---O1W$^{\#1}$, O9—H9---O16 and N6—H6A---O11$^{\#5}$.

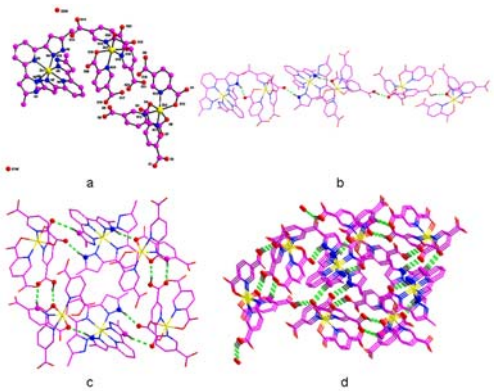

Fig. 5 The molecular structure of supramolecular complex **4** (a); A view of 1D chain via hydrogen bonds (b); A view of 2D layer via hydrogen bonds (c); A view of 3D supramolecular network structure via hydrogen bonds (d).

Comparison of the structures The structural analysis indicates that Cadmium and Zinc atom in supramolecular complexes **1-4** are all six-coordinated modes with core of ZnN6, ZnO2N4 and ZnO3N3, respectively, forming a slightly distorted-octahedral geometry. H_2L is in the form of μ_1–η^1–η^1–η^1 to coordination with metal Cd and Zn in supramolecular complexes **1-4**, which are same as the coordination mode of complex $[Zn(H_2L^2)(H_2O)_2](SO_4)\cdot 0.87H_2O$ in the literature[36], and different from the coordination mode(μ_2–η^1–η^1–η^1–η^1) of complex $[Zn_2(HL^2)_2(\mu_2\text{-}SO_4)]\cdot 2H_2O$ in the literature[36]. The 2,6-H_2pdc acts as pincer tridentate chelate ligand in the form of μ_1–η^1–η^1–η^1 coordination mode in supramolecular complex **3**. While the 2,5-H_2pdc ligand is in the form of μ_1–η^1–η^1 coordination mode in supramolecular complex **4**. The order of the corresponding bond lengths of M-N (M = Cd, Zn) are M-$N_{pyridine}$ < M-$N_{pyrazolyl}$ in the supramolecular complexes **2-4**, which are same as order of corresponding length in the complex $[Zn(H_2L^2)(H_2O)_2](SO_4)\cdot 0.87H_2O$[36]. The order of the corresponding bond length of Zn-N in carboxylate ligands is Zn-$N_{2,6\text{-}H2pdc}$ < Zn-$N_{2,5\text{-}H2pdc}$ for supramolecular complexes **3** and **4**. However, the order of the corresponding bond length of Zn-O in carboxylate ligands is Zn-$O_{2,5\text{-}H2pdc}$ < Zn-$O_{2,6\text{-}H2pdc}$. In complex **3**, the bond lengths of Zn−$N_{pyridine}$ is 2.0729(18) Å, which is similar to that of the complex $[Zn(H_2L^2)(H_2O)_2](SO_4)\cdot 0.87H_2O$[36]. Moreover, the average bond lengths Zn−$N_{pyrazolyl}$ is 2.204(7) Å, which is a little bit bigger than 2.176(9) Å of the complex $[Zn(H_2L^2)(H_2O)_2](SO_4)\cdot 0.87H_2O$[36]. In addition, in the H_2L ligand, pyrazolyl rings from two sides are distorted to the least-squares plane (central pyridyl ring) with dihedral angles of supramolecular complexes **1-4**, in which these dihedral angles are in the range of 0.14(1.18)-10.95(0.32)°. The torsion angles between the coordination carboxyl and center metal in supramolecular complexes **3** and **4** are different. In supramolecular complex **3**, the torsion angles are in the range of 0.26(0.29)~1.45(0.31)° (ZnO3C20C19 and ZnO2C15C14), and the torsion angles between the coordination carboxyl and metal in supramolecular complex **4** are in the range of -0.96(1.02)~26.30(1.02)° (Zn3O19C61C60 and Zn3O16C54C53). It may be caused by different distorted degrees of the carboxyl groups from carboxlyate ligands.

Spectroscopic characterization

IR spectral studies For supramolecular complex **1**, a broad absorption band appearing at 3417 cm^{-1} indicates the presence of the water molecules. Absorption bands at 3191 and 3127 cm^{-1} were assigned to the stretching vibrations of the N-H in the pyrazolyl rings and the C-H stretching vibrations of the pyridine/pyrazolyl rings, respectively. Weak absorptions bands observed at 2932 and 2859 cm^{-1} are features of the C–H vibration modes of -CH_3 groups. The bands at 1609, 1582, 1447, 1283, and 1011 cm^{-1} are attributed to the characteristic stretching vibrations of the pyrazolyl and pyridine rings. In addition, the detailed appointments of the IR spectra data for supramolecular complexes **1-4** are listed in **Table 3**.

Table 3 The detailed attribution of IR (cm^{-1}) for supramolecular complexes **1-4**.

Complex	**1**	**2**	**3**	**4**
$\nu_{(O\text{-}H)}$	3417	3437	3456	3445
$\nu_{(N\text{-}H)}$	3191	3195	3136	3167
$\nu_{(Ar\text{-}H)}$	3127	3128	3085	3025
$\nu_{as(-CH3)}$	2932, 2859	2925, 2858,	2929, 2858	2923, 2853
pyridine/ pyrazolyl	1609, 1582, 1447, 1293, 1011	1581, 1508, 1446, 1326, 1014	1519, 1446, 1290, 1253, 1018	1559, 1508, 1457, 1261, 1038
$\nu_{as(COO^-)}$	-	-	1620	1640
$\nu_{s(COO^-)}$	-	-	1380	1399

UV-visible spectra The electronic absorption spectra of supramolecular complexes **1-4** were recorded at the room temperature in the form of the solid sample. As shown in **Table 3**, electronic absorption spectra of **1-4** have similar absorption patterns. The high-frequency absorption bands at 258-278 nm for **1-4** are assigned to π-π* transition of the H_2L ligand. There were slightly red shifts as compared with the absorption bands of 256 nm from the free H_2L ligand. Similarly, the absorption bands at 340 nm for **1**, 338 nm for **2**, 342 nm for **3** and 364 nm for **4** exhibit slightly red shifts as compared with the absorption band of 336 nm from the free H_2L ligand.

Table 4 Characteristic UV-vis absorption bands (nm) of complexes **1-4**.

Complex	π–π*	LLCT
1	210, 260	340
2	216, 258	338
3	218, 278	342
4	210, 278	364

XRD analysis The powder X-ray diffraction data of the four supramolecular complexes were obtained and compared with the corresponding simulated single-crystal diffraction data (**Fig. S7-S10**). All the peaks presented in the measured patterns closely match with the simulated patterns generated from the single crystal diffraction data, which indicates that **1-4** are in pure phase.

Thermal properties To examine the thermal stability of the synthesized supramolecular complexes, thermal gravimetric analysis (TG) was carried out at a heating rate of 10 ºC/min under N2 atomosphere in the temperature range of 20-1000 ºC. As shown in **Fig. 6** and **Fig. 7**, the TG curves of these four supramolecular complexes are slightly different owing to the differences of their structures. In **1**, the result shows the initial weight loss of 4.26% before 60 ºC is due to the release of the two free H_2O molecules (calc 4.79%). The second weight loss occurred in the range of 60-323 ºC, with a percentage weight loss of 17.64% which is ascribed to the release of the free NO_3^- (calc 16.51%). The third weight loss occurred in the temperature of 323-643 ºC, with a percentage 48.38%, which was ascribed to the release of one H_2L ligand (calc 46.86%). The last step of decomposition occurred within the range of 643-1000 ºC, which is considered the loss of remaining H_2L ligand, and the final residue is corresponds to CdO. The TG curve of **2** is similar to **1**. The first weight loss of 5.56% before 53 ºC was attributed to the reduction of two lattice water molecule. The second weight loss occurs in the temperature range of 53-242 ºC, with a percentage weight loss of 3.55%, which is ascribed to the release of lattice EtOH molecule. The third weight loss occurred in the temperature of 242-593 ºC, with a percentage 53.4%, which was ascribed to the release of one H_2L ligand (calc 54.01%). The last step of decomposition occurred within the range of 593-1000 ºC, which is considered the loss of remaining H_2L ligand, and the final residue was corresponds to CdO. The TG curve of 3 shows five stages. The initial weight loss of 1.46% before 34 ºC is attributed to the release of lattice water molecule. The second weight loss of 3.93% in the temperature range of 34-114 ºC is due to the release of lattice EtOH molecule. The third step was observed in 114-268 ºC, with a percentage weight loss of 33.37%, which was considered the loss of free one and a half 2,6-H_2pdc molecules. The fourth weight loss of 20.33% in the temperature range of 268-390 ºC was attributed to the release of one 2,6-H_2pdc ligand. The last step of decomposition occurred within the range of 390-1000 ºC, which was considered the loss of remaining H_2L ligand, and the final residue was corresponds to ZnO. The TG curve of **4** can be divided into four stages. The initial weight loss of 1.47% before 43 ºC is due to the release of one and a half free H_2O molecule. The second weight loss of 3.92% in the temperature range of 43-88 ºC is according to the release of CH_3^- moiety. The third step was observed in 88-323 ºC with a percentage weight loss of 68.54%, which was considered the loss of six 2,5-H_2pdc ligands and two pyridines. The last step of decomposition occurred within the range of 323-1000 ºC, which was considered the loss of remaining pyrazole, and the final residue was corresponds to ZnO.

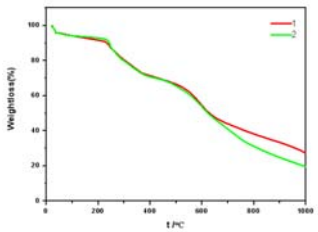

Fig. 6 The TG curves for supramolecular complexes **1** and **2**.

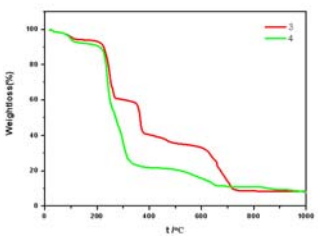

Fig. 7 The TG curves for supramolecular complexes **3** and **4**.

Photoluminescent Properties The solid-state photoluminescent spectra of supramolecular complexes **1-4** at room temperature were examined, respectively. As shown in **Fig S11-S14**, **1** displays a broad emission band at 386 nm upon excitation at 293 nm with a slit width (3:3). Similar to **1**, **2** also exhibits a broad emission peak at 364 nm upon excitation at 301 nm with a slit width (3:3). When excited at 342 nm, the emission maximum was at 397 nm for **3**, with the same slit width (3:1). **4** displays a broad emission band at 420 nm upon excitation at 364 nm with a slit width (3:3).

By comparing the emission wavelengths of supramolecular complexes **1-4**, it is found that the emission of **1** occurs to red-shift in contrast to **2**, which is probably due to the different composition of the complexes. Similarly, the emission of 4 occurs to red-shift in contrast to **3**, which is probably due to the different coordinated structures.

Biological activity

MTT Cell viability was measured using the MTT assay on 96-well plates in PC12 cells and hADSCs (**Fig. 8**). The IC_{50} values of these complexes were fit by the linear regression models of these complexes (**Table 5**). The viability of PC12 cells and hADSCs exposed to supramolecular complexes at different concentrations was significantly decreased as compared with the control group. The results show that the cytotoxic phenomena become gradually distinct. And incubation of PC12 cells and hADSCs with different concentrations of supramolecular complexes for 24 h or 48 h resulted in dose-dependent decreases in cell viability. Further, the percentage of viable cells of 24 h was higher than that of 48 h.

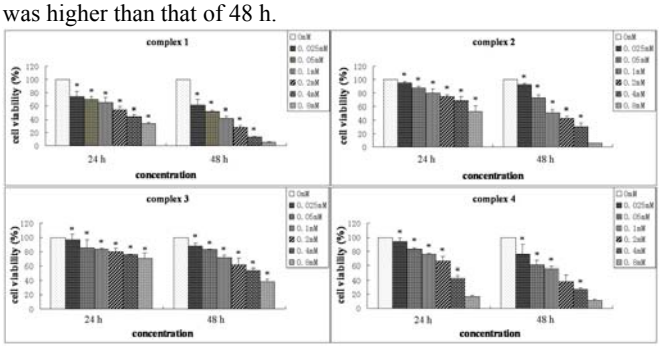

Fig. 8 Cell viability of the hADSCs assayed by MTT. Data are means ± SD of triplicate determinations.

Table 5 The IC_{50} (mM) values of complexes **1-4** in PC12 cells and hADSCs

Cell type	1	2	3	4
PC12	0.26 ± 0.02	0.87 ± 0.02	2.13 ± 0.01	0.27 ± 0.02
hADSCs	0.33 ± 0.01	0.95 ± 0.02	1.98 ± 0.02	0.31 ± 0.01

Cell apoptosis Apoptosis is a major mode of cell death in response to cytotoxic drug treatment[37]. To evaluate the induction of apoptosis, we stained cells, treated with the concentrations of 0.025, 0.1, 0.4 and 1.6 mM of the drugs with Annexin-V FITC and PI. Following drug treatment for 48 h, hADSCs were dually stained with Annexin V-FITC and PI and analyzed by FACS.

For supramolecular complex **1**, the flowcytometric analysis revealed that the apoptotic population of cells was 12.416% (0.025 mM), 44.382% (0.1 mM), 52.765% (0.4 mM) and 76.989% (1.6 mM), respectively, as compared to the respective controls (3.637%) (**Fig. 9**). Taken together, these results also corroborate that the death induced by drugs follows apoptotic pathway.

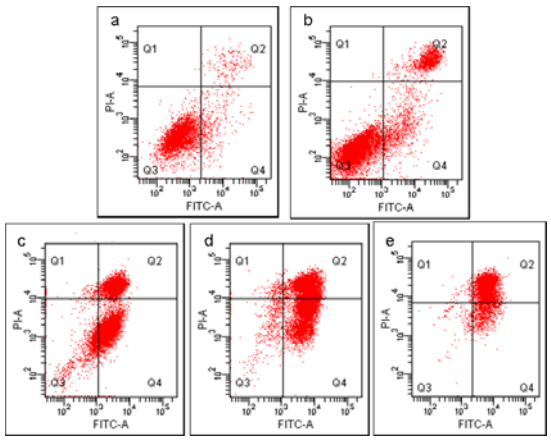

Fig. 9 Quantification of apoptosis by annexin V binding to hADSCs. Cells were incubated with supramolecular complexes under different concentration and then stained with annexin V-FITC/PI and analyzed by flow cytometry. Untreated cells (a), 0.025 mM (b), 0.1 mM (c), 0.4mM (d) and 1.6 mM (e) of supramolecular complex **1**. The lower right quadrant of each cytometry scatter plot shows the annexin V+PI− cells; the upper right quadrant shows the annexin V+PI+ cells. Data represent the mean calculated from three independent experiments.

Staining for apoptosis assay It's a great convenience estimating the population of apoptosis and neurons with double staining method by Acridine orange (AO) and ethidium bromide (EB).

In this work, cell nuclei for control group were performed natural morphological with spherical or ellipsoidal. Their cell boundaries were clear, and nuclei emitted bright green fluorescence while almost invisible red fluorescence. However, for experimental group, the density was significantly lower with the increasing of the concentration of complexes. Cell nucleus performed irregularly spherical morphology, and appeared apoptotic bodies which were observed bead-like bodies for different sizes, with gradually weakened green fluorescent and increased red fluorescence. These apoptotic bodies showed smooth and clear edges, consistent and uniform fluorescence. Meanwhile, with gradually increasing of the concentration of complexes, typical fibroblast-like morphology for hADSCs disappeared. Cell became shrinkage and deformation, desquamated from the bottom of the flasks, showing apoptosis features and necrosis properties (**Fig. 10**).

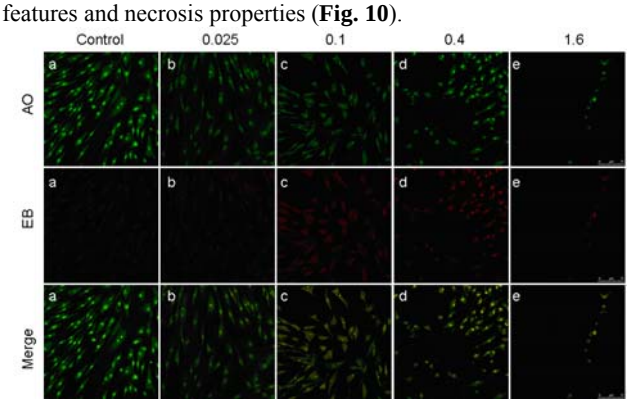

Fig. 10 Human ADSCs were stained by AO/EB and observed under fluorescence microscopy. Cells without treatment (a),

0.025 mM complex **1** (b), 0.1 mM complex **1** (c), 0.4 mM complex **1** (d) and 1.6 mM complex **1** (e). Images shown are acquired from a fluorescent microscope at a magnification of 200×.

Conclusions

Four new supramolecular complexes with H_2L as ligand have been synthesized and characterized by elemental analysis, IR and UV-vis spectroscopy and X-ray crystal diffraction analysis. In addition, the biological activity of the complexes was evaluated by MTT and apoptosis assay. The results show that the cytotoxicity of complex **3** is lower than those of **1**, **2** and **4**. In particular, the apoptotic phenomenon for PC12 cell is more obvious, when the concentration is larger than 0.26 mM for complex **1** (0.87mM for **2**, 2.13 mM for **3**, 0.27 mM for **4**). Meantime, so is the apoptotic phenomenon for hADSCs, when the concentration is larger than 0.33 mM for complex **1** (0.95mM for **2**, 1.98 mM for **3**, 0.31 mM for **4**).

Abbreviations

H_2L	2,6-di-(5-methyl-1H-pyrazol-3-yl)pyridine
2,6-H_2pdc	2,6- pyridinedicarboxylic acid
2,5-H_2pdc	2,5-pyridinedicarboxylic acid
hADSCs	stem cells derived from human adipocyte
MTT	3-(4,5-dimethylthiazol-2-yl)-2,5-diphenyltetrazolium bromide
LLCT	ligand-to-ligand charge transfer
TG	thermal gravimetric analysis
DMF	dimethylformamide
PBS	phosphate-buffered saline
AO	acridine orange
EB	ethidium bromide
PI	propidium iodide

Notes and references

[a] *Regenerative Medicine Centre, First Affiliated Hospital of Dalian Medical University, No. 222 Zhongshan Road, Dalian, 116011, PR China. Fax: +86 411 84394568; Tel: +86 411 84394568; E-mail: liujing.dlrmc@hotmail.com*

[b] *College of Chemistry and Chemical Engineering, Liaoning Normal University, No. 850, Huanghe Road, Dalian, 116029, PR China. Fax: +86 411 82156987; Tel: +86 411 82156987; E-mail: xingyongheng2000@163.com*

† Electronic Supplementary Information (ESI) available: This work was supported by the grants of the National Natural Science Foundation of China (No.21071071, No. 21371086), and State key Laboratory of Inorgnic Synthesis and Preparative Chemistry, Jilin University, Changchun 130012, P. R. China (Grant No. 2013-05); the Chinese National Natural Science Foundation (No. 81071009, 30801061) and the International S&T Cooperation Project of the Ministry of S&T of China (No. 2010DFR30850).

‡ Tables of atomic coordinates, an isotropic thermal parameters, and complete bond distances and angles have been deposited with the Cambridge Crystallographic Data Center. Copies of this information may be obtained free of charge, by quoting the publication citation and deposition numbers CCDC: 954129 for **1**, 954130 for **2**, 954131 for **3** and 954132 for **4** from the Director, CCDC, 12 Union Road, Cambridge, CB2 1EZ, UK (fax: +44–1223–336033; E–mail: deposit@ccdc.cam.ac.uk or http://www.ccdc.cam.ac.uk).

1 M.X. Li, M. Yang, J.Y. Niu, L.Z. Zhang and S.Q. Xie, Inorg. Chem., 2012, 51, 12521-12526; M.X. Li, D. Zhang, L.Z. Zhang, J.Y. Niu and B.S. Ji, J. Organomet. Chem., 2011, 696, 852-858; M.X. Li, L.Z. Zhang, M. Yang, J.Y. Niu and J. Zhou, Bioorg. Med. Chem. Lett., 2012, 22, 2418-2423; Y. Sun, W. Guo and M. Du, Inorg. Chem. Commun., 2011, 14, 873-876; M.X. Li, Y.L.Lu, M. Yang, Y.K. Li, L.Z. Zhang and S.Q. Xie, Dalton Trans., 2012, 41, 12882-12887; M.X. Li, L.Z. Zhang, C.L. Chen, J.Y. Niu and B.S. Ji, J. Inorg. Biochem., 2012, 106, 117-125; X.Y. Yi, H.C. Fang, Z.G. Gu, Z.Y. Zhou, Y.P. Cai, J. Tian and P.K. Thallapally, Cryst. Growth Des., 2011, 11, 2824-2828; R. Feng, L. Chen, Q.H. Chen, X.C. Shan, Y.L. Gai, F.L. Jiang and M.C. Hong, Cryst. Growth Des., 2011, 11, 1705-1712; Y.N. Zhang, P. Liu, Y.Y. Wang, L.Y. Wu, L.Y. Pang and Q.Z. Shi, Cryst. Growth Des., 2011, 11, 1531-1541.

2 L.L. Xu, C.J. Zheng, L.P. Sun, J. Miao and H.R. Piao, Eur. J. Med. Chem., 2012, 48, 174-178; A.A. Bekhit, H.M.A. Ashour, Y.S. Abdel Ghany, A.E.A. Bekhit and A. Baraka, Eur. J. Med. Chem., 2008, 43, 456-463; F.A. Ragab, N.M. Abdel Gawad, H.H. Georgey and M.F. Said, Eur. J. Med. Chem., 2013, 63, 645-654; A.M. Vijesh , A.M. Isloor, P. Shetty, S. Sundershan and H.K. Fun, Eur. J. Med. Chem., 2013, 62, 410-415.

3 S.L. Zhu, Y. Wu, C.J. Liu, C.Y. Wei, J.C. Tao and H.M. Liu, Eur. J. Med. Chem., 2013, 65, 70-82; G.M. Nitulescu, C. Draghici and A.V. Missir, Eur. J. Med. Chem., 2010, 45, 4914-4919.

4 D. Braga and F. Grepioni, Acc. Chem. Res., 2000, 33, 601-608; P.D. Beer and E.J. Hayes, Coord. Chem. Rev., 2003, 240, 167-189; P.D. Beer and S.R. Bayly, Top. Curr. Chem., 2005, 255, 125-162; S.G. Galbraith and P.A. Tasker, Supramol. Chem., 2005, 17, 191-207.

5 T.D. Roberts, F. Tuna, T.L. Malkin, C.A. Kilner and M.A. Halcrow, Chem. Sci., 2012, 3, 349-354; A.X. Zheng, H.F. Wang, C.N. Lu, Z.G. Ren, H.X. Li and J.P. Lang, Dalton Trans., 2012, 41, 558-566; E. Coronado, J.R. Galán Mascarós, M.C. Giménez-López, M. Almeida and J.C. Waerenborgh, Polyhedron, 2007, 26, 1838-1844.

6 E. Coronado, M.C. Gimimenez-Lopez, C. Gimenez-Saiz and F.M. Romero, CrystEngComm., 2009, 11, 2198-2203; L.T. Ghoochany, S. Farsadpour, Y. Sun and W.R. Thiel, Eur. J. Inorg. Chem., 2011, 23, 3431-3437.

7 P. Wang, C.H. Leung, D.L. Ma, S.C. Yan and C. M. Che, Chem. Eur. J., 2010, 16, 6900-6911; L. Wang, Q. Yang, H. Chen and R.X. Li, Inorg. Chem. Commun., 2011, 14, 1884-1888.

8 A.T. Çolak, F. Çolak, O.Z. Yeşilel and O. Büyükgüngör, J. Mol. Struct., 2009, 936, 67-74.

9 T.A. Sliemandagger and W.L. Nicholson, Appl. Environ. Microbiol., 2001, 67, 1274-1279; J.R.H. Xie, V.H. Smitth Jr. and R.E. Allen, Chem. Phys., 2006, 322, 254-268.

10 H.T. Xu, N.W. Zheng, H.H. Xu, Y.G. Wu, R.Y. Yang, E.Y. Ye and X.L. Jin, J. Mol. Struct., 2001, 597, 1-5.

11 E.E. Sileo, O.E. Piro, G.R. Miguel, A. Blesa, A.S. de Araujo and E.E. Castellano, Struct. Chem., 2008, 19, 651-657.

12 H. Tucker and D.F. Thomas, J. Med. Chem., 1992, 35, 804-807.

13 P. Sengupta, S. Ghosh and T.C.W. Mak, Polyhedron, 2001, 20, 975-980.

14 G. Süss-Fink, L.G. Cuervo, B. Therrien, H. Stoeckli-Evans and G.B. Shul'pin, Inorg. Chim. Acta, 2004, 357, 475-484.

15 Y.S. Song, B. Yan and Z.X. Chen, J. Coord. Chem., 2005, 58, 811-816; G.Q. Zhang, Q. Wang, Y. Qian, G.Q. Yang and J.S. Ma, J. Mol. Struct., 2006, 796, 187-194.

16 Y.S. Song, B. Yan and Z.X. Chen, J. Mol. Struct., 2005, 750, 101-108; M. Yang, L. Wang, G.H. Li, L. Yang, Z. Shi and S.H. Feng, J. Alloys Compd., 2007, 440, 57-61.

17 K. Akhbari and A. Morsali, J. Mol. Struct., 2008, 878, 65-70.

18 B. Zhao, X.Y. Chen, P. Cheng, D.Z. Liao, S.P. Yan and Z.H. Jiang, J. Am. Chem. Soc., 2004, 126, 15394-15395; B. Zhao, P. Cheng, X.Y. Chen, C. Cheng, W. Shi, D.Z. Liao, S.P. Yan and Z.H. Jiang, J. Am. Chem. Soc., 2004, 126, 3012-3013.

19 M.B. Zhang, J. Zhang, S.T. Zheng and G.Y. Yang, Angew. Chem., Int. Ed., 2005, 44, 1385-1388; J.Y. Lu and A.M. Babb, Chem. Commun., 2003, 12, 1346-1347.

20 C. Brouca-Cabarrecq, A. Fernandes, J. Jaud and J.P. Costes, Inorg. Chim. Acta, 2002, 332, 54-60.

21 K. Singh, Y. Kumar, P. Puri, M. Kumar and C. Sharma, Eur. J. Med. Chem., 2012, 52, 313-321; T. Srdić-Rajić, M. Zec, T. Todorović, K. AnCelković and S. Radulović, Eur. J. Med. Chem., 2011, 46, 3734-3747.

22 G.A. Gauna, J. Marino, M.C. García Vior, L.P. Roguin and J. Awruch, Eur. J. Med. Chem., 2011, 46, 5532-5539; P.J. Rani and S. Thirumaran, Eur. J. Med. Chem., 2013, 62, 139-147.

23 S.K. Hanson, R.T. Baker, J.C. Gordon, B.L. Scott, A.D. Sutton and D.L. Thorn, J. Am. Chem. Soc., 2009, 131, 428-429; M.O. Guerrero-Pérez, J.M. Rosas, R. López-Medina, M.A. Bañares, J. Rodríguez-Mirasol and T. Cordero, Catal. Commun., 2011, 12, 989-992.

24 G. Centi, P. Lanzafame and S. Perathoner, Catal. Today., 2011, 167, 14-30; E.J. Gao, T.D. Sun, S.H. Liu, S. Ma, Z, Wen, Y, Wang, M.C. Zhu, L. Wang, X.N. Gao, F. Guan, M.J. Guo and F.C. Liu, Eur. J. Med. Chem., 2010, 45, 4531-4538.

25 M.M. Aly, Y.A. Mohamed, K.A.M. El-Bayouki, W.M. Basyouni and S.Y. Abbas, Eur. J. Med. Chem., 2010, 45, 3365-3373.

26 B.M. Strem, K.C. Hicok, M. Zhu, I. Wulur, Z. Alfonso, R.E. Schreiber, J.K. Fraser and M.H. Hedrick, Keio J. Med., 2005, 54, 132-141.

27 Y.M. Yang, S.K. Gupta, K.J. Kim, B.E. Powers, A. Cerqueira, B.J. Wainger, H.D. Ngo, K.A. Rosowski, P.A. Schein, C.A. Ackeifi, A.C. Arvanites, L.S. Davidow, C.J. Woolf and L.L. Rubin, Cell Stem Cell, 2013, 12, 713-726.

28 L.A. Greene and A.S. Tischler, Proc. Natl. Acad. Sci., 1976, 73, 2424-2428.

29 M.H. Wu, S.B. Huang, Z.F. Cui, Z. Cui and G.B. Lee, Sensors and Actuators B, 2008, 129, 231-240; M.H. Wu, J.P.G. Urban, Z. Cui and Z.F. Cui, Biomed. Microdevices, 2006, 8, 331-340; Z.F. Cui , X. Xu , N. Trainor , J.T. Triffitt , J.P.G. Urban and U.K. Tirlapur, Toxicol. in Vitro, 2007, 21, 1318-1324.

30 M.A. Halcrow, Coord. Chem. Rev., 2005, 249, 2880-2908; Y.M. Luo, Z. Chen, R.R. Tang and L.X. Xiao, Chem. React. Eng. Techno., 2006, 5, 549-553; Y.M. Luo, L.X. Xiao, Z. Chen, W. Huang and X.C. Tang, Chem. Res. Appl., 2008, 3, 299-303.

31 G.M. Sheldrick, SADABS, Program for Empirical Absorption Correction of Area Detector Data, University of Göttingen, Göttingen, Germany, 1996.

32 G.M. Sheldrick, SHELXS 97, Program for Crystal Structure and Refinement, University of Göttingen, Göttingen, Germany, 1997.

33 H.D. Flack, Acta Cryst., 1983, A39, 876-881.

34 T. Mosmann, J. Immunol. Methods, 1983, 65, 55-63.

35 D.L. Spector, R.D. Goldman, L.A. Leinwand (Eds), Cells: a laboratory manual, in Cold Spring Harbor, Cold Spring Harbor Laboratory Press, New York, 1998.

36 L.J. Wan, C.S. Zhang, Y.H. Xing, Z. Li, N. Xing, L.Y. Wan and H. Shan, Inorg. Chem., 2012, 51, 6517-6528.

37 I. Vermes, C. Haanen, H. Steens-Nakken and C. Reutelingsperger, J. Immunol. Methods, 1995, 184, 39-51.